NTNU

Norwegian University of
Science and Technology

TMT4320 Nanomaterials
Septemeber 28th, 2016

- TNN5:Characterization of nanomaterials: XRD, SAXS, EDX, EELS, Nanoindentation

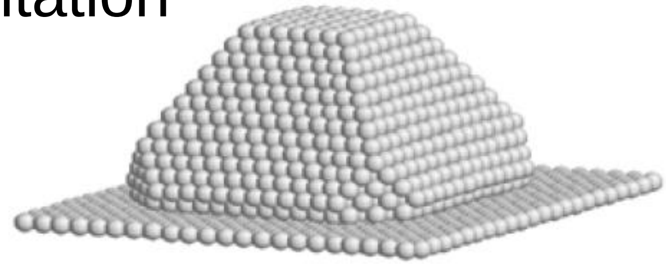

Last lecture

- Summary of:
  - Bottom-up synthesis: Physical/Vapour phase methods
  - Characterization of nanomaterials: TEM, SEM and XPS
- Characterization of Nanomaterials: STM, AFM, XRD and SAXS

Last lecture

- Characterization of Nanomaterials: STM and AFM
  - Near field microscopy techniques:
    - Scanning tunneling microscopy (STM)
      - Tunnel effect
      - Very thin tip electrically powered → tear the electrons by tunnel effect
      - Measuring electric current → Reconstruct where the electrons are

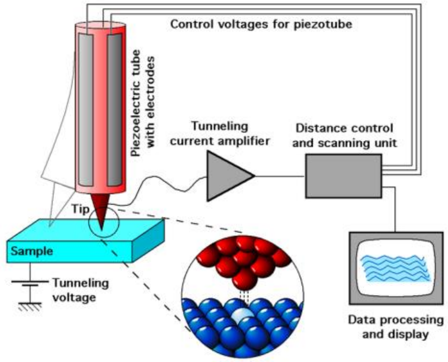

Last lecture

- Characterization of Nanomaterials: STM and AFM

  - Near field microscopy techniques:
    - Atomic Force Microscopy (AFM)
      - Surface sensing technique → Attractive vs Repulsive → Interatomic forces
      - Detection method: Laser beam → Reflexion when cantilever deflects

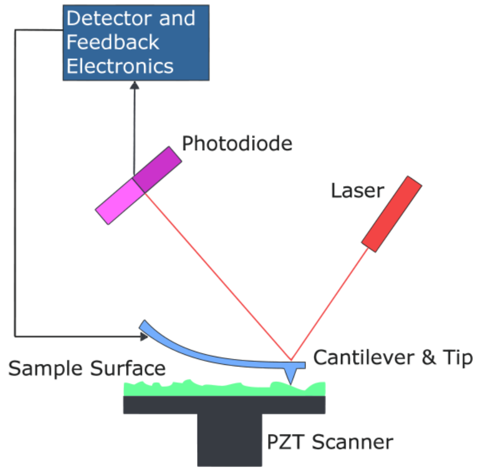

Last lecture

- Characterization of Nanomaterials: STM and AFM

  - Near field microscopy techniques:
    - Atomic Force Microscopy (AFM)
      - Three types:
        - Contact mode (repulsive forces)
        - Non contact mode (attractive forces)
        - Tapping mode. Non contact mode with larger amplitudes (both repulsive and attractive forces). Larger resolution
        - AFM vs TEM: Convolution effect

        Tip shape influence

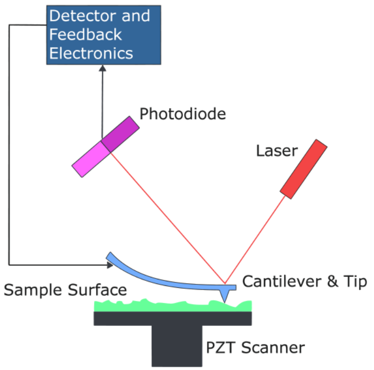

Today lecture

- Characterization of Nanomaterials: XRD, SAXS, EDX, EELS, FIM, 3DAP, Nanoindentation

  - X-Ray Diffraction (XRD)
  - Small angle X-Ray scattering (SAXS)
  - Energy Dispersive X-Ray Spectroscopy (EDS/EDX)
  - Electron loss energy spectroscopy (EELS)
  - Field Ion Microscope (FIM)
  - Three-dimensional atom probe (3DAP)
  - Nanoindentation

X-ray diffraction

Technique to study the structure, defects and stresses of solids

Beam of x-ray with wavelength from 0.07 to 0.2 nm is diffracted by crystalline specimen according to Bragg's law:

$\lambda = 2\, d \sin \theta$

λ= X-Ray wavelength
θ = diffraction angle
d = interplanar distance

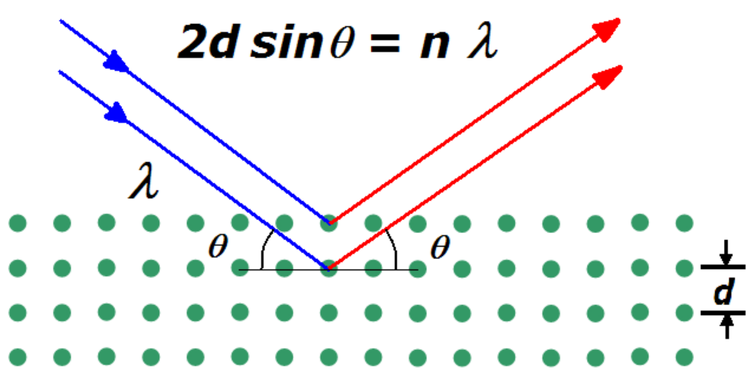

X-ray diffraction

Identify crystalline phases

Structural characteristics (cell parameters, crystallite sizes, defects, etc)

Non-destructive technique

Sample preparation is easy

Cheap

X-ray diffraction

Detection of homogenous and inhomogenous strains due to their dependence on the Bragg angle

Homogeneous or uniform elastic strain shits the diffraction peaks, without change in peak profile. Shift change in the peaks means change in the lattice constants.

Inhomogeneous strains vary from crystallite to crystallite or even within a single crystallite. As XRD is an averaged information leads to peak broadening.

Peak broadening can also be due to reduction of crystallite size. This can be determined by peak profile analysis → Rietveld refinements

X-ray diffraction

- Grazing Incidence Small Angle X-Ray Scattering (GISAXS)
  - To a first approximation: average height *h*, average size *d*, average separation *D*

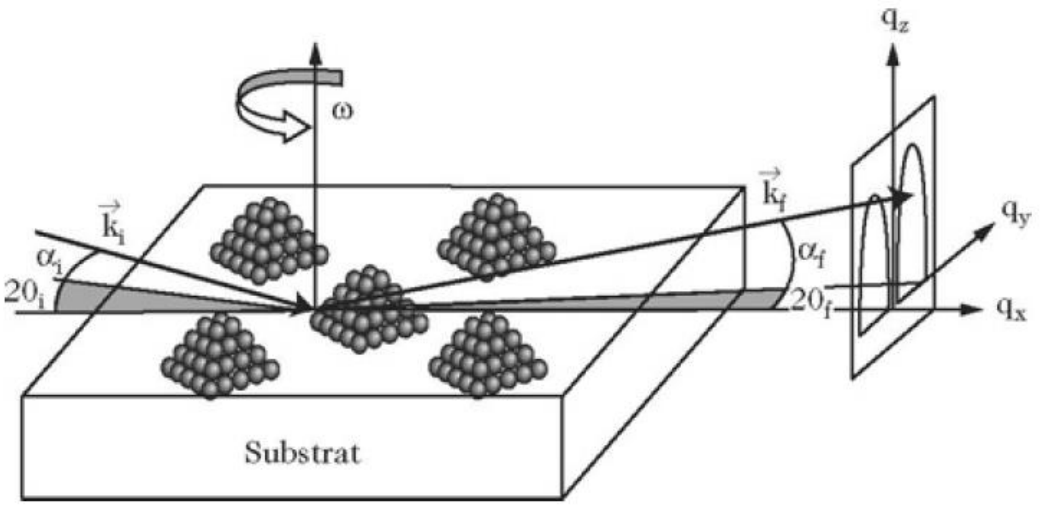

X-ray diffraction: instruments

Different sources : Cu, Mo, Co, synchrotron

Different sample holders: air-sensitive, shape, temperature dependent

Different detectors and filters

XRD lab at DMSE (IMT)

D8 Advance : High Temperature

Da Vinci 1

Da Vinci 2

A Unit

D8 Focus

XRD lab at DMSE (IMT)

D8 Advance : High Temperature

- High/Low temperature/pressure

MRI TC-Wide Range camera
Vacuum, inert or reactive gas atmospheres
-190-400 °C with LT stage
RT-1200 °C with a choice of two radiant heaters
RT-1400 °C with Pt-Rh or Ta strip heaters
0-20 bar gas pressure

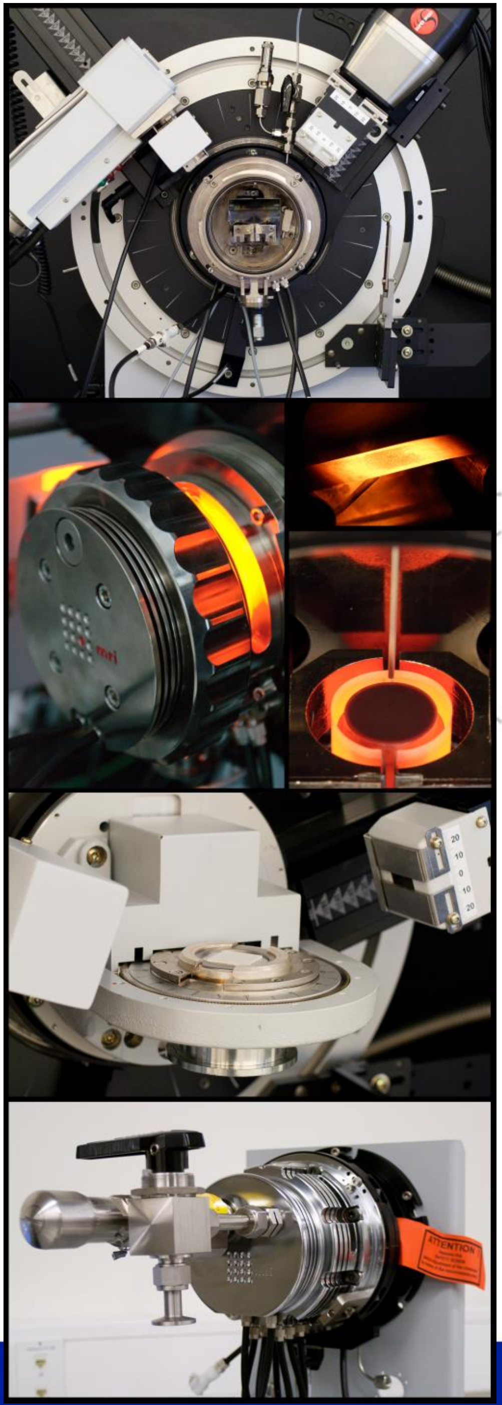

XRD lab at DMSE (IMT)

Da Vinci 1

CuKα radiation
2.5° primary and secondary Soller slits
60-90 position sample changer
LynxEye™ SuperSpeed Detector
Variable divergence slit: "V6" means that the divergence slit (the slit between the X-ray source and the sample) opens automatically such that the illuminated length on the sample always remains 6 mm (when using fixed divergence slit, the illuminated length on the sample changes from long to short - this is just geometry).

XRD lab at DMSE (IMT)

Da Vinci 1

- Well suited for:
  - Fast XRD scans for phase identification
  - Samples that can wait in a queue for hours before being measured (the engineer will load the samples into the instrument every morning and afternoon)
  - Energy-discriminating detector makes it useful also for the fluorescing elements (Fe, Co, Mn)
- Not so good for:
  - Samples that change fast in air (then the D8 Focus may be better to use, due to the booking system)
  - Samples that doesn't fit the standard sample holders
  - Measurements where you want to avoid the Kα2 contributions (then the A-unit is recommended)

XRD lab at DMSE (IMT)

Da Vinci 1

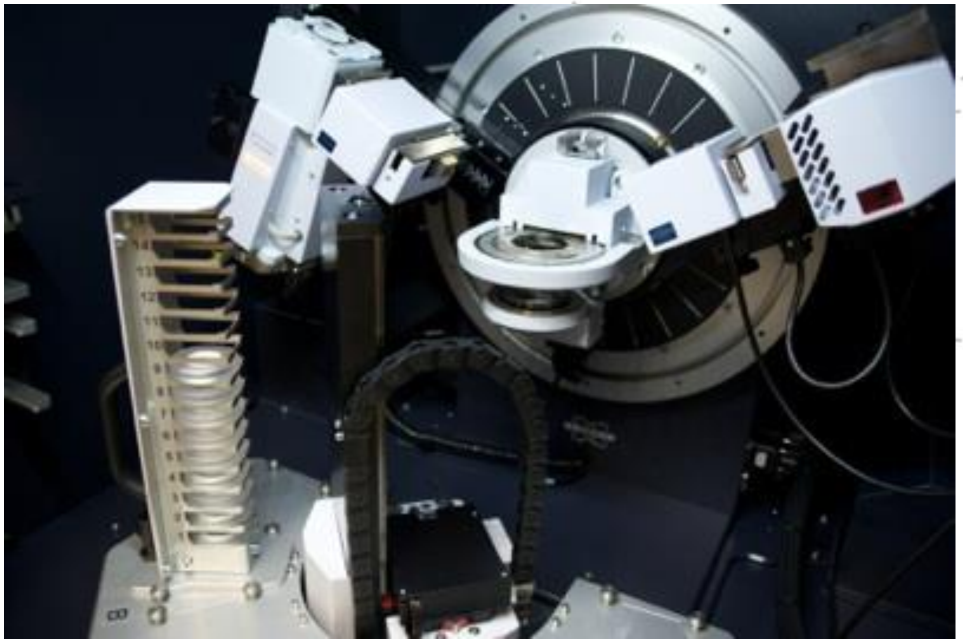

XRD lab at DMSE (IMT)

Da Vinci 2

MoKα radiation
Capillary sample stage
Typically 3-155 degrees 2θ (0.46 Å-1 < Q < 17.3 Å-1, 13.6 Å > d > 0.36 Å)

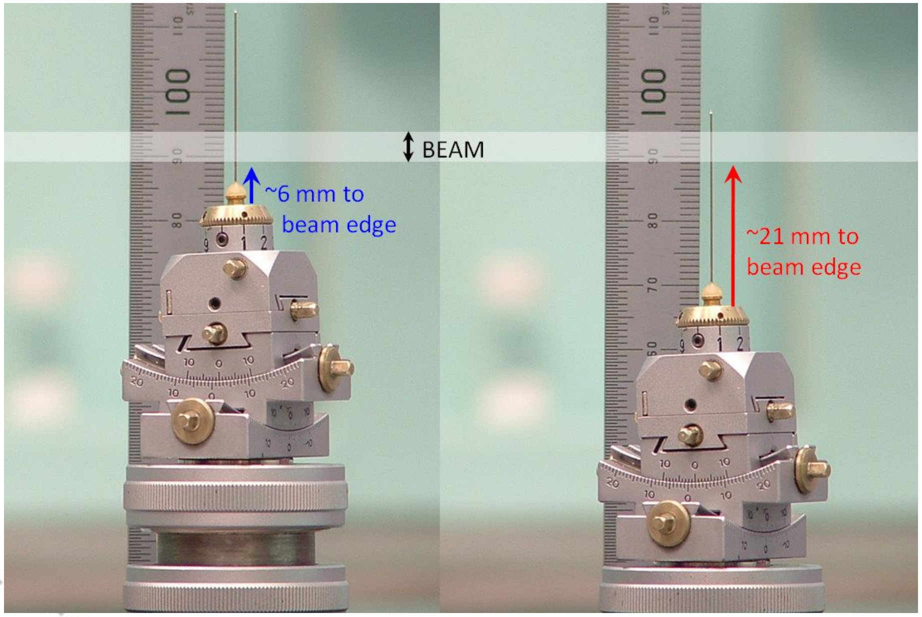

XRD lab at DMSE (IMT)

- A Unit

- Bragg-Brentano geometry
- Data collection from 0.5 to 140° 2θ
- Quartz primary monochromator
- Cu Kα1 radiation
- Rotating single sample holder with user selectable rotation speeds

- Well suited for:

- Collection of data for structure solution and/or Rietveld refinement

- Not so good for:

- Samples containing fluorescing elements (Fe, Co, Mn), depending on the concentration.

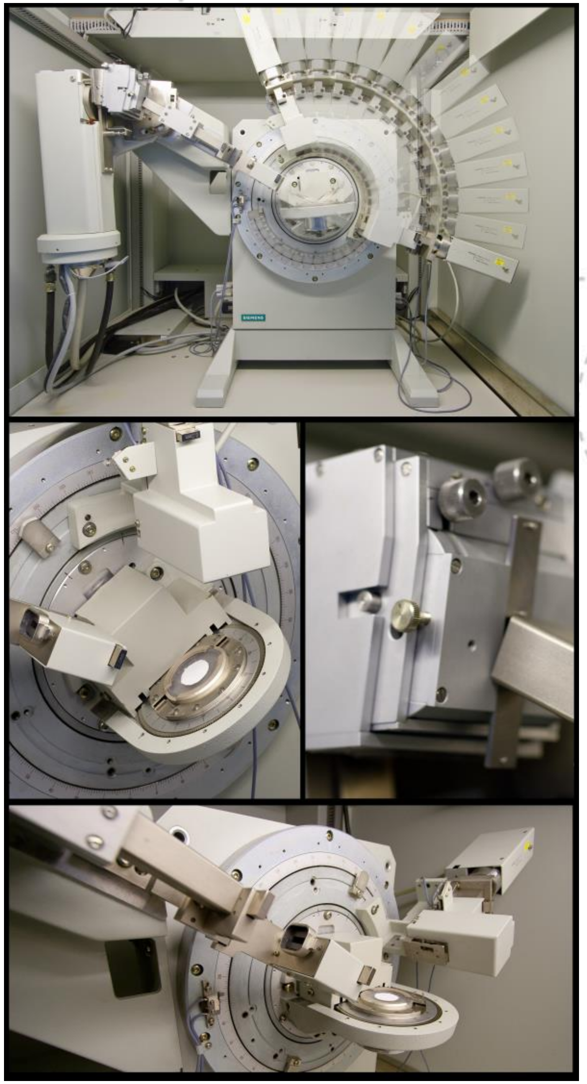

XRD lab at DMSE (IMT)

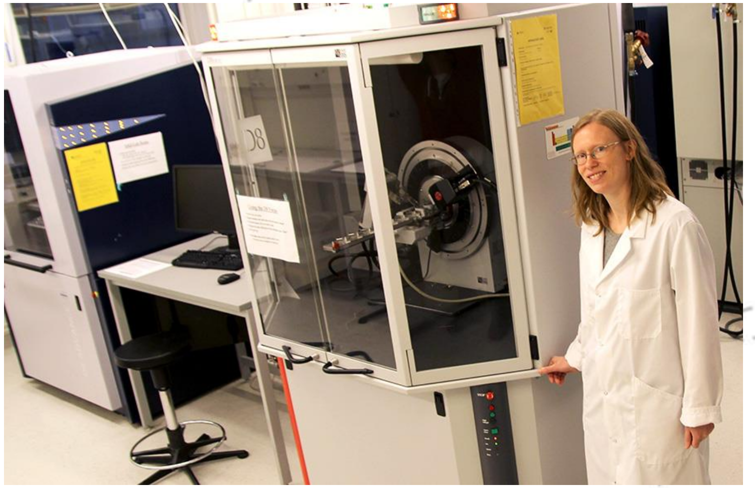

- D8 Focus
  - Bragg-Brentano geometry
  - θ–2θ operating mode
  - Cu Kα radiation
  - 9 position sample changer
- Well suited for:
  - Booking system - useful if you wish to measure your samples straight after production etc.
- Not so good for:
  - Samples containing cobalt (due to fluorescence). Then the Da Vinci 1 is recommended since its detector has better energy discrimination.

Lay. Double Perov. vs Single Perov.

Ln**Ba*****M*****$_2$O$_6$;** *Ln* = lanthanide, Y; *M* = Co, Fe, Mn. **vs. *Ln*$_{0.5}$Ba$_{0.5}$*M*O$_3$**

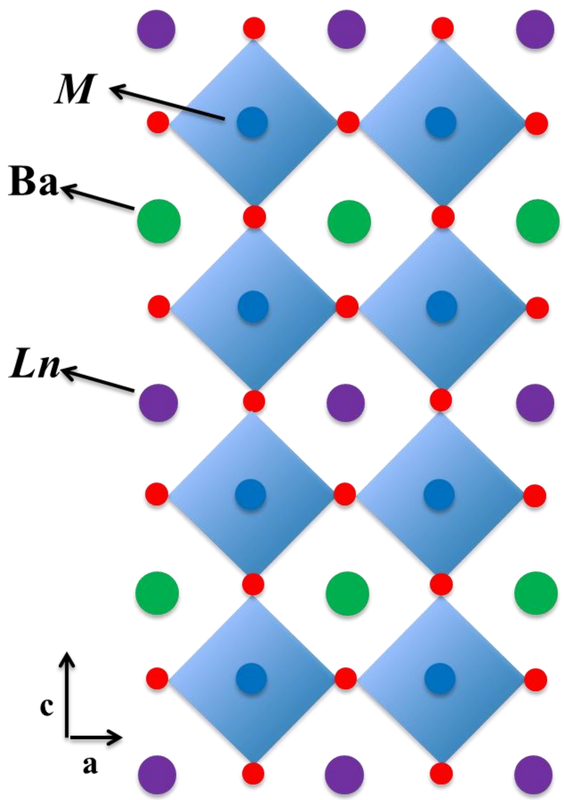

Ln**Ba*****M*****$_2$O$_6$**

LDP: A-site cation order

Tetragonal

$\rightleftharpoons$

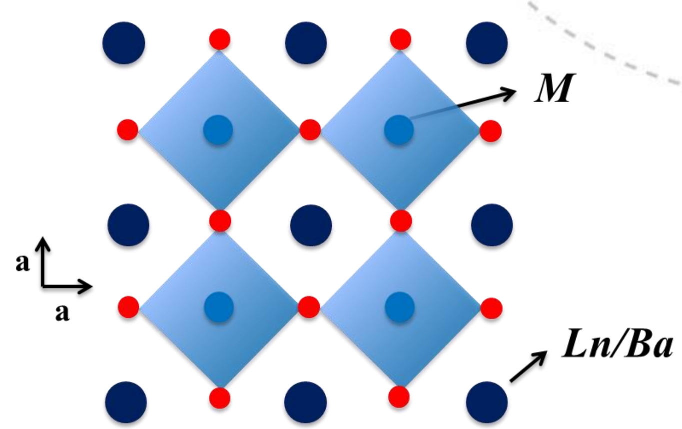

Ln**$_{0.5}$Ba$_{0.5}$*M*O$_3$**

SP: A-site cation disorder

Cubic

Why? → Oxygen vacancies

O^{2-} ion and e^- conduction

Ba presence good for H^+ conduction

Synthesis

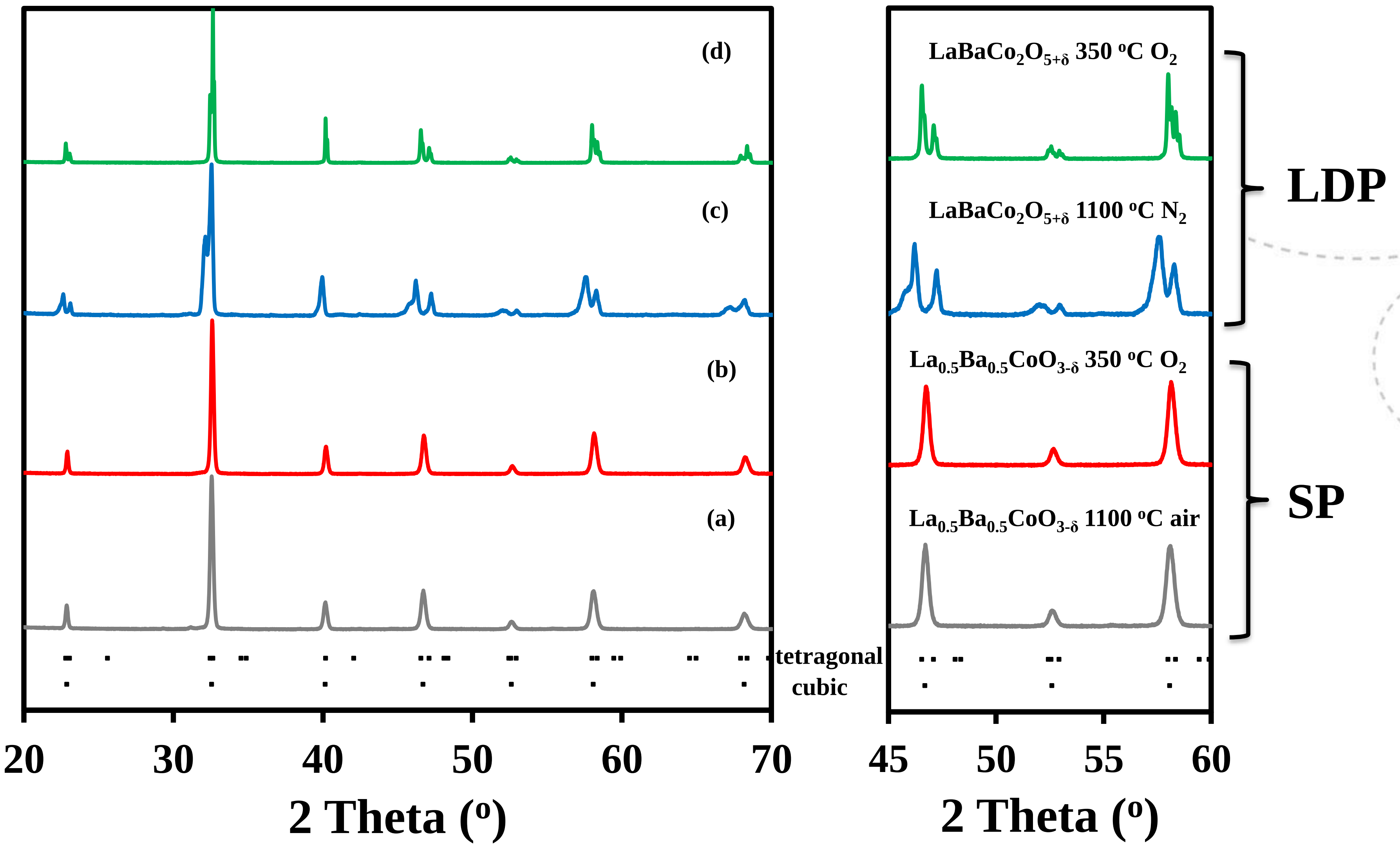
(d)
(c)
(b)
(a)
tetragonal
cubic
20
30
40
50
60
70
2 Theta (°)
LaBaCo2O5+δ 350 °C O2
LaBaCo2O5+δ 1100 °C N2
La0.5Ba0.5CoO3-δ 350 °C O2
La0.5Ba0.5CoO3-δ 1100 °C air
45
50
55
60
2 Theta (°)
LDP
SP

EDS/EDX

Electron Dispersive X-Ray Spectroscopy (EDS/EDX)

Analytical technique used for the elemental analysis or chemical characterization

Attached to SEM and TEM microscopes

Limitation on element accuracy → Heavier elements more accurate than lighter elements → Diffraction technique.

Interaction of electrons with matter

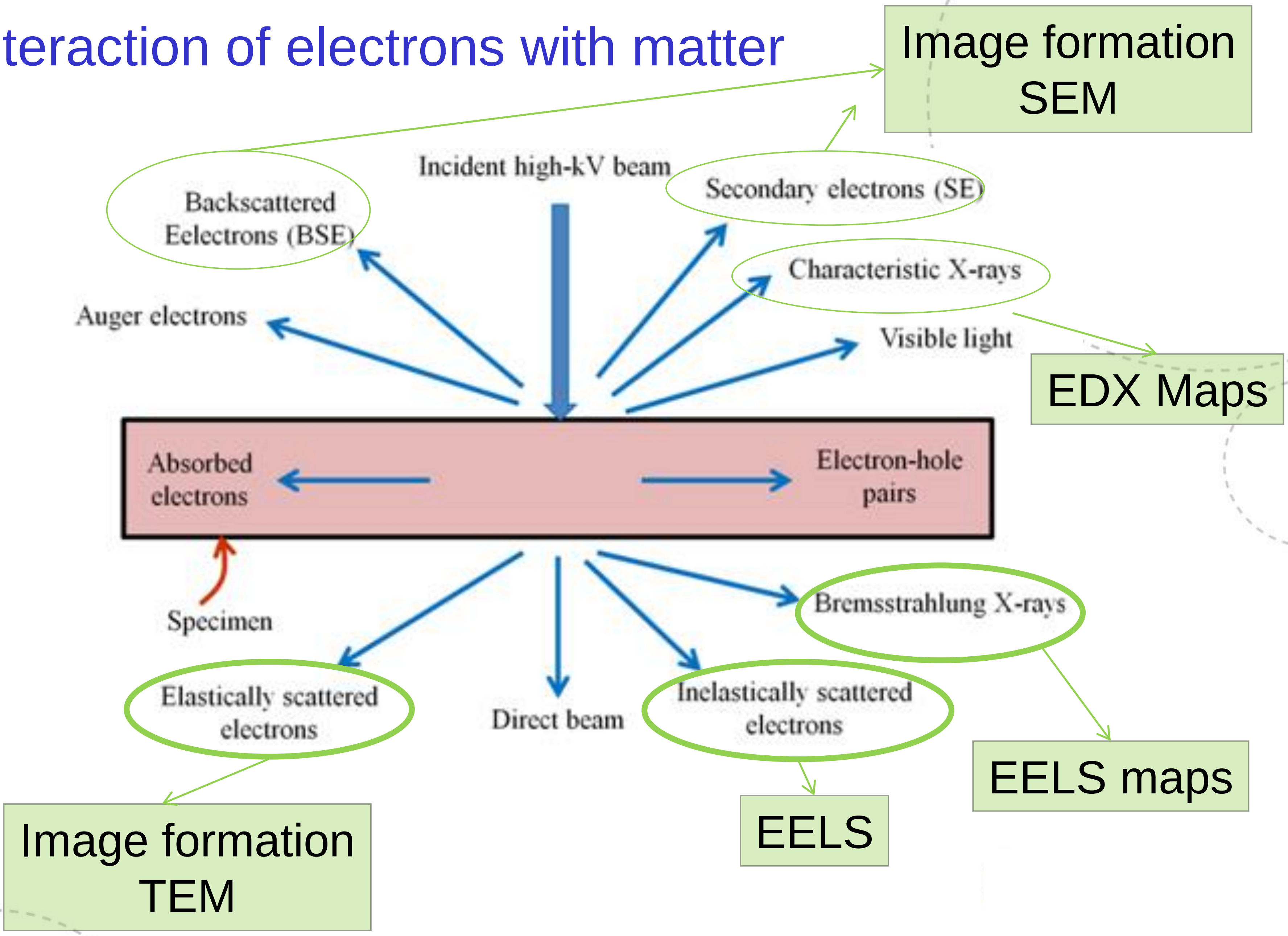

Scanning Electron Microscopy SEM

- ❖ Image formation is because of the secondary and back-scattered Electrons
- ❖ Samples are dehydrated and made conductive.

EDX unit

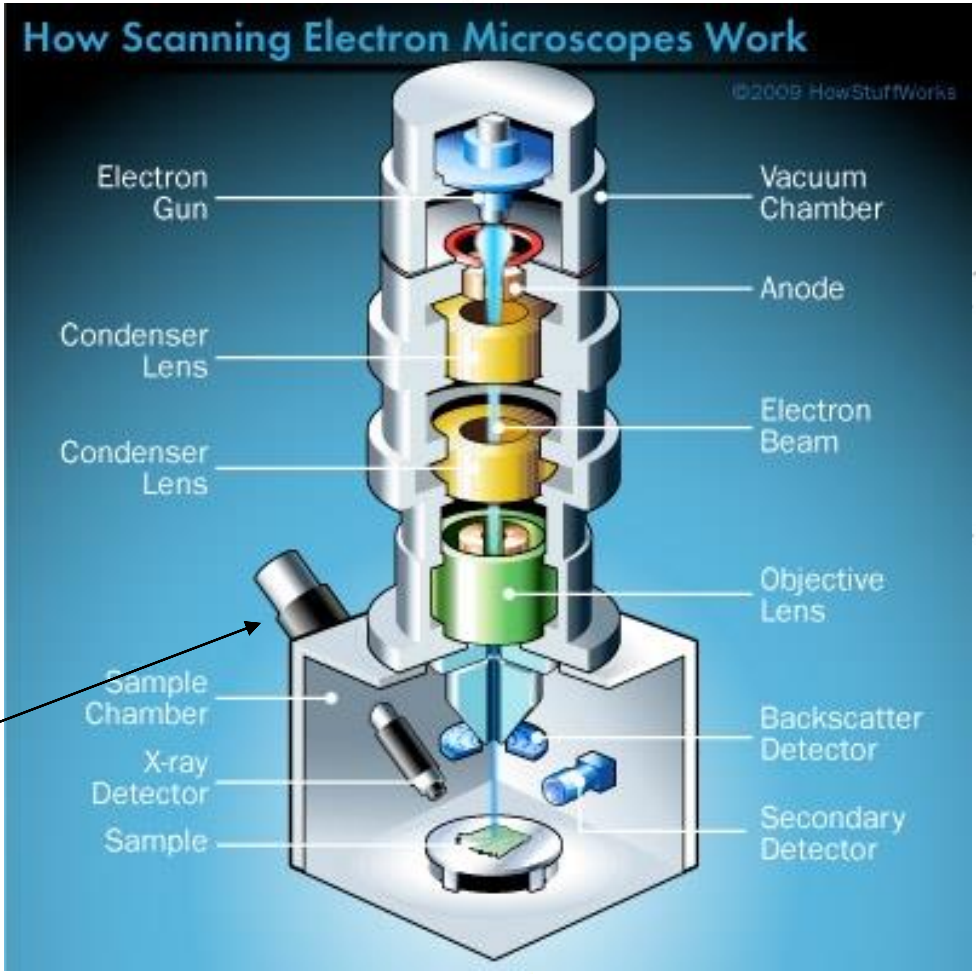

http://science.howstuffworks.com/scanning-electron-microscope2.htm

EDS/EDX

Electron Dispersive X-Ray Spectroscopy (EDS/EDX)

Example:

Journal of
Materials Chemistry A

ROYAL SOCIETY OF CHEMISTRY

PAPER

View Article Online
View Journal | View Issue

Cite this: *J. Mater. Chem. A*, 2014, 2, 11114

Insight into surface segregation and chromium deposition on $La_{0.6}Sr_{0.4}Co_{0.2}Fe_{0.8}O_{3-\delta}$ cathodes of solid oxide fuel cells

Ling Zhao,[a] John Drennan,[b] Chun Kong,[c] Sudath Amarasinghe[d] and San Ping Jiang*[a]

$La_{0.6}Sr_{0.4}Co_{0.2}Fe_{0.8}O_{3-\delta}$, (LSCF) perovskite oxide is one of the most important cathode materials in the development of intermediate temperature solid oxide fuel cells (IT-SOFCs), but vulnerable to chromium deposition and poisoning in the presence of gaseous chromium species from the chromia-forming metallic interconnect. Despite extensive studies on Cr deposition on SOFC cathode materials, there is a lack of direct evidence on the surface chemistry and Cr deposition. Here, the fundamental relationship between the surface segregation and Cr deposition of LSCF cathodes is studied on dense LSCF bar samples using a dual beam high resolution focused ion beam (FIB) and a high resolution scanning electron microscope coupled with EDS. FIB-EDS mapping results clearly indicate the segregation of SrO

EDS/EDX

Journal of
Materials Chemistry A

ROYAL SOCIETY OF CHEMISTRY

PAPER

View Article Online
View Journal | View Issue

Insight into surface segregation and chromium deposition on $La_{0.6}Sr_{0.4}Co_{0.2}Fe_{0.8}O_{3-\delta}$ cathodes of solid oxide fuel cells

Cite this: J. Mater. Chem. A, 2014, 2, 11114

Ling Zhao,[a] John Drennan,[b] Chun Kong,[c] Sudath Amarasinghe[d] and San Ping Jiang*[a]

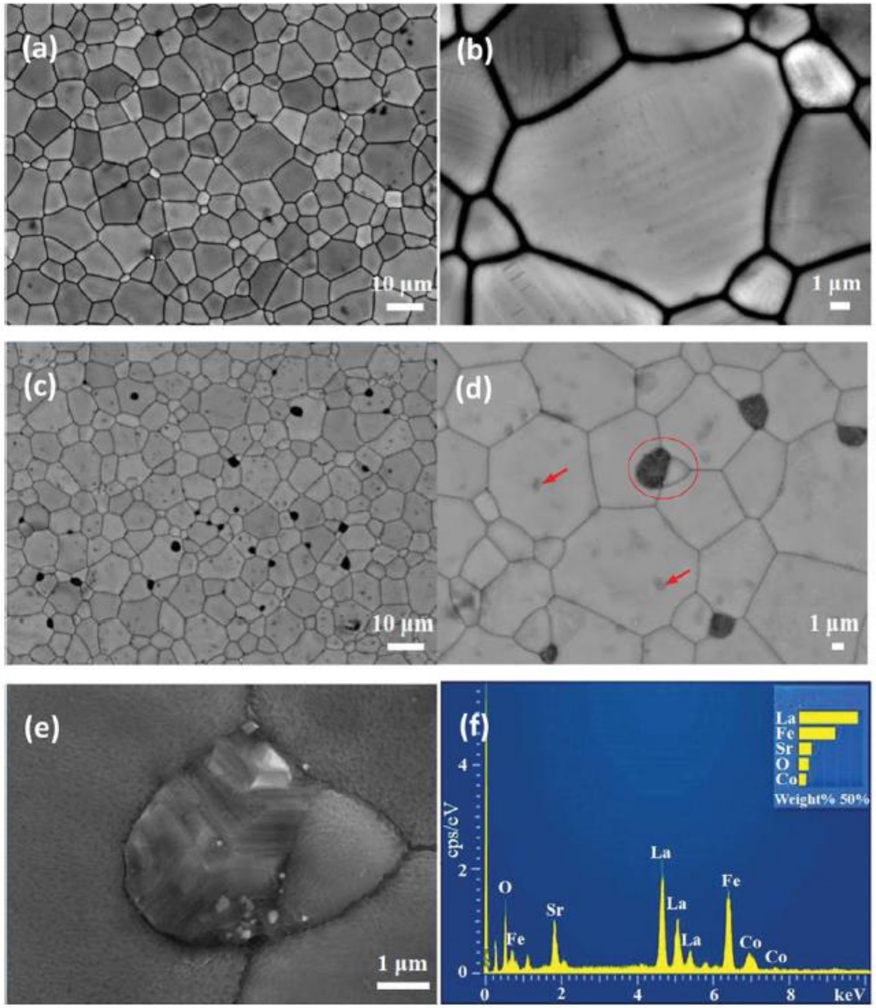

Fig. 2 SEM micrographs of (a and b) the freshly prepared LSCF and (c and d) LSCF samples after being heat treated at 800 °C in the absence of Cr_2O_3 in air for 96 h; (e) enlarged image of the segregated micron-sized particle as circled in (d); and (f) typical EDS spectrum of LSCF grains in (b). Arrows in (d) indicate segregated isolated submicron-sized particles.

EDS/EDX

Journal of
Materials Chemistry A

ROYAL SOCIETY OF CHEMISTRY

PAPER

View Article Online
View Journal | View Issue

Cite this: J. Mater. Chem. A, 2014, 2, 11114

Insight into surface segregation and chromium deposition on $La_{0.6}Sr_{0.4}Co_{0.2}Fe_{0.8}O_{3-\delta}$ cathodes of solid oxide fuel cells

Ling Zhao,[a] John Drennan,[b] Chun Kong,[c] Sudath Amarasinghe[d] and San Ping Jiang[*a]

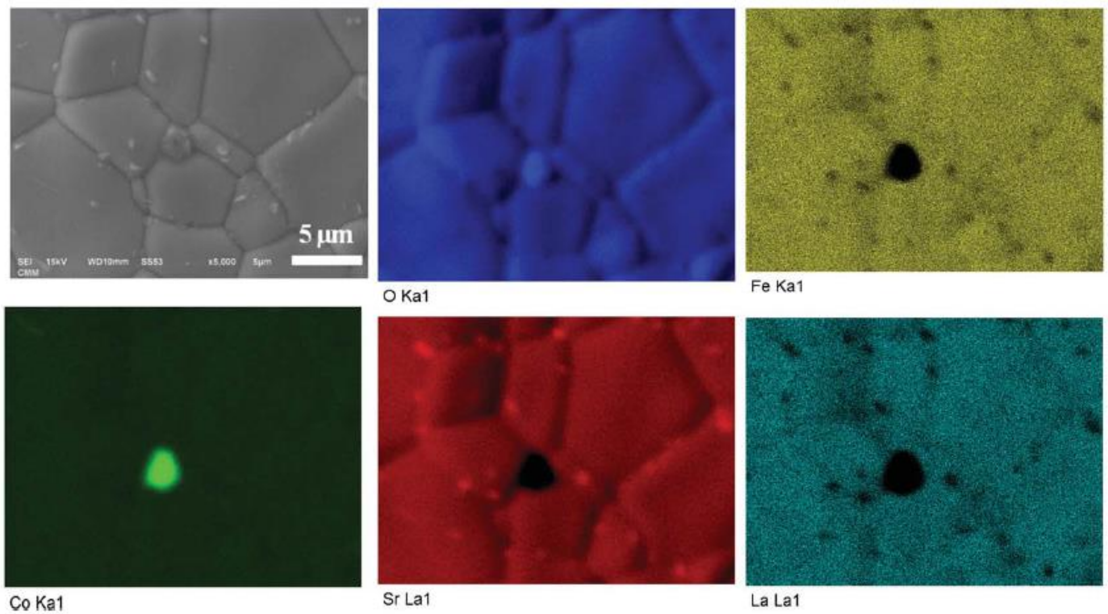

Fig. 3 SEM micrograph and EDS mapping of the LSCF surface after being heat-treated in the absence of Cr_2O_3 at 800 °C in dry air for 96 h.

EELS

Electron Energy Loss Spectroscopy (EELS)

Technique very close to EDX → Analyze chemical compositions

It works better for lighter elements than EDX

Attached to a TEM unit → Scattered electrons

Interaction of electrons with matter

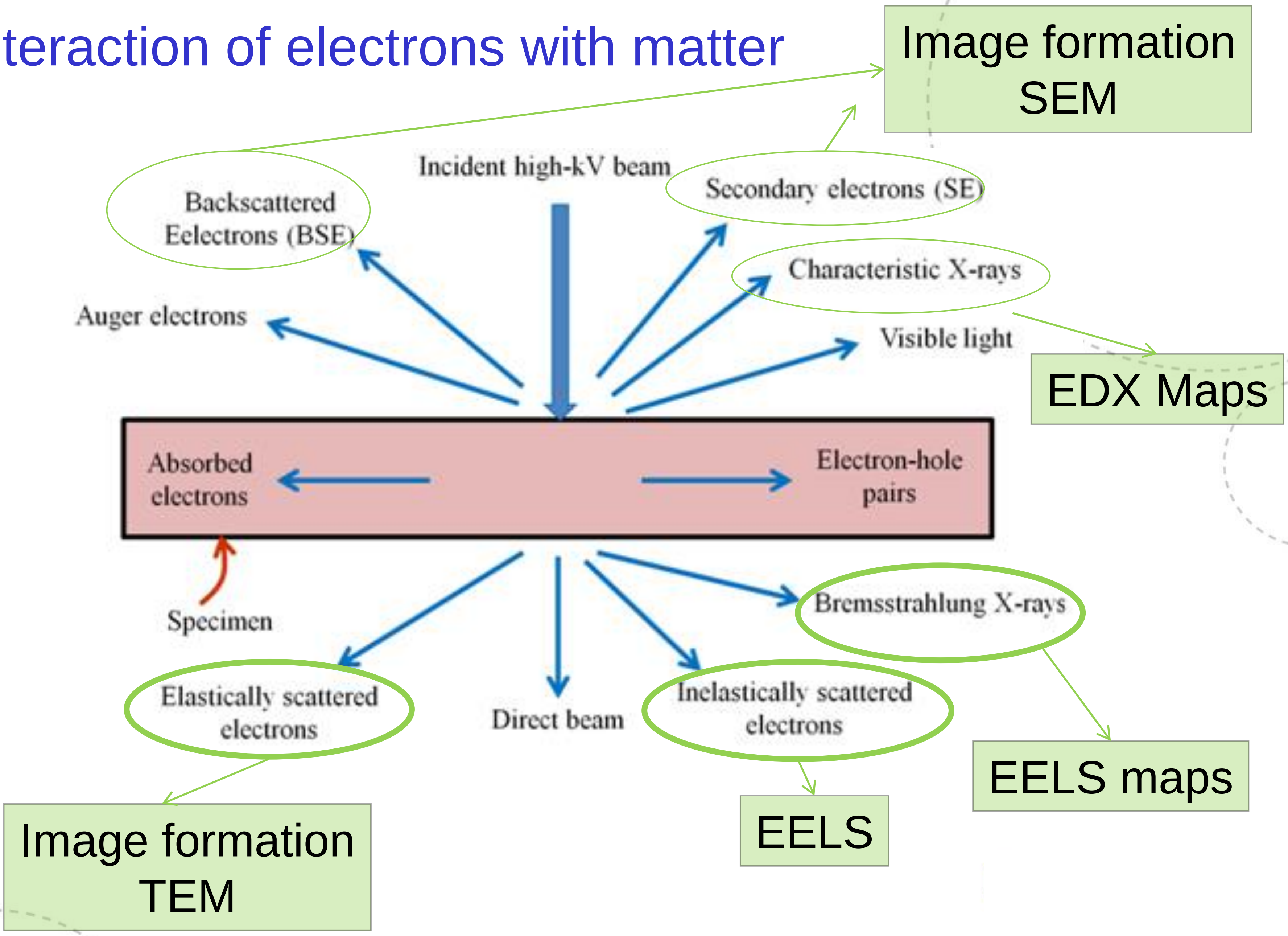

EELS

Electron Energy Loss Spectroscopy (EELS) @ NTNU

EELS

Electron Energy Loss Spectroscopy (EELS)

Example

CHEMISTRY OF MATERIALS

Article

pubs.acs.org/cm

Nanoscale Ordering in Oxygen Deficient Quintuple Perovskite $Sm_{2-\varepsilon}Ba_{3+\varepsilon}Fe_5O_{15-\delta}$: Implication for Magnetism and Oxygen Stoichiometry

Nadezhda E. Volkova,[†] Oleg I. Lebedev,[‡] Ludmila Ya. Gavrilova,[†] Stuart Turner,[§] Nicolas Gauquelin,[§] Md. Motin Seikh,[‡,∥] Vincent Caignaert,[‡] Vladimir A. Cherepanov,[*,†] Bernard Raveau,[*,‡] and Gustaaf Van Tendeloo[§]

EELS

CHEMISTRY OF MATERIALS
Article
pubs.acs.org/cm

Nanoscale Ordering in Oxygen Deficient Quintuple Perovskite $Sm_{2-\varepsilon}Ba_{3+\varepsilon}Fe_5O_{15-\delta}$: Implication for Magnetism and Oxygen Stoichiometry

Nadezhda E. Volkova,[†] Oleg I. Lebedev,[‡] Ludmila Ya. Gavrilova,[†] Stuart Turner,[§] Nicolas Gauquelin,[§] Md. Motin Seikh,[‡,∥] Vincent Caignaert,[‡] Vladimir A. Cherepanov,[*,†] Bernard Raveau,[*,‡] and Gustaaf Van Tendeloo[§]

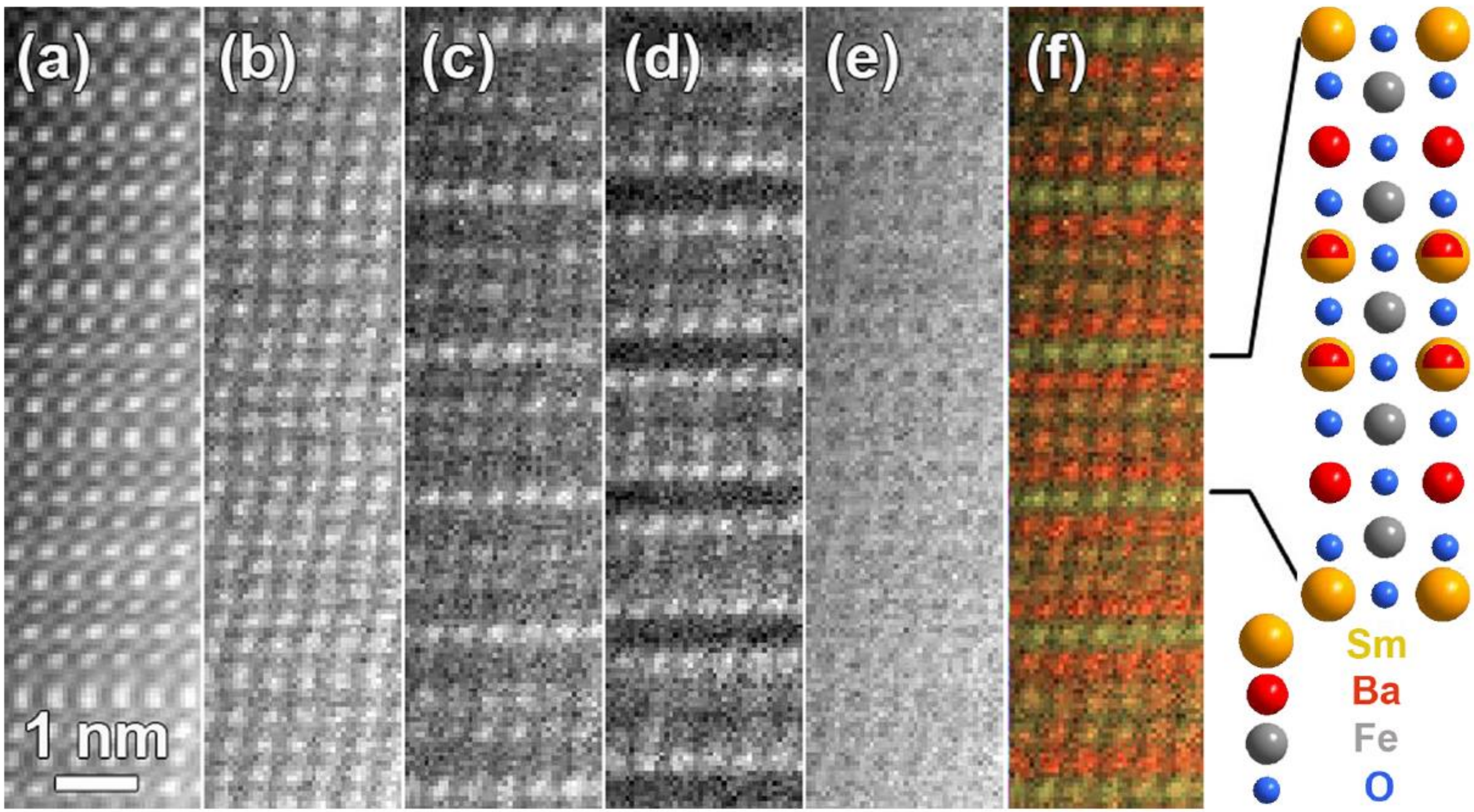

Figure 4. EELS elemental mapping of $Sm_{2-\varepsilon}Ba_{3+\varepsilon}Fe_5O_{15-\delta}$. (a) Overview HAADF-STEM image, (b) Fe-$L_{2,3}$ map, (c) Sm-$M_{4,5}$ map, (d) Ba-$M_{4,5}$ map, (e) O−K map, and (f) color overlay with Sm in yellow and Ba in red together with a structural model.

EELS

CHEMISTRY OF MATERIALS
Article
pubs.acs.org/cm

Nanoscale Ordering in Oxygen Deficient Quintuple Perovskite $Sm_{2-\varepsilon}Ba_{3+\varepsilon}Fe_5O_{15-\delta}$: Implication for Magnetism and Oxygen Stoichiometry

Nadezhda E. Volkova,[†] Oleg I. Lebedev,[‡] Ludmila Ya. Gavrilova,[†] Stuart Turner,[§] Nicolas Gauquelin,[§] Md. Motin Seikh,[‡,∥] Vincent Caignaert,[‡] Vladimir A. Cherepanov,[*,†] Bernard Raveau,[*,‡] and Gustaaf Van Tendeloo[§]

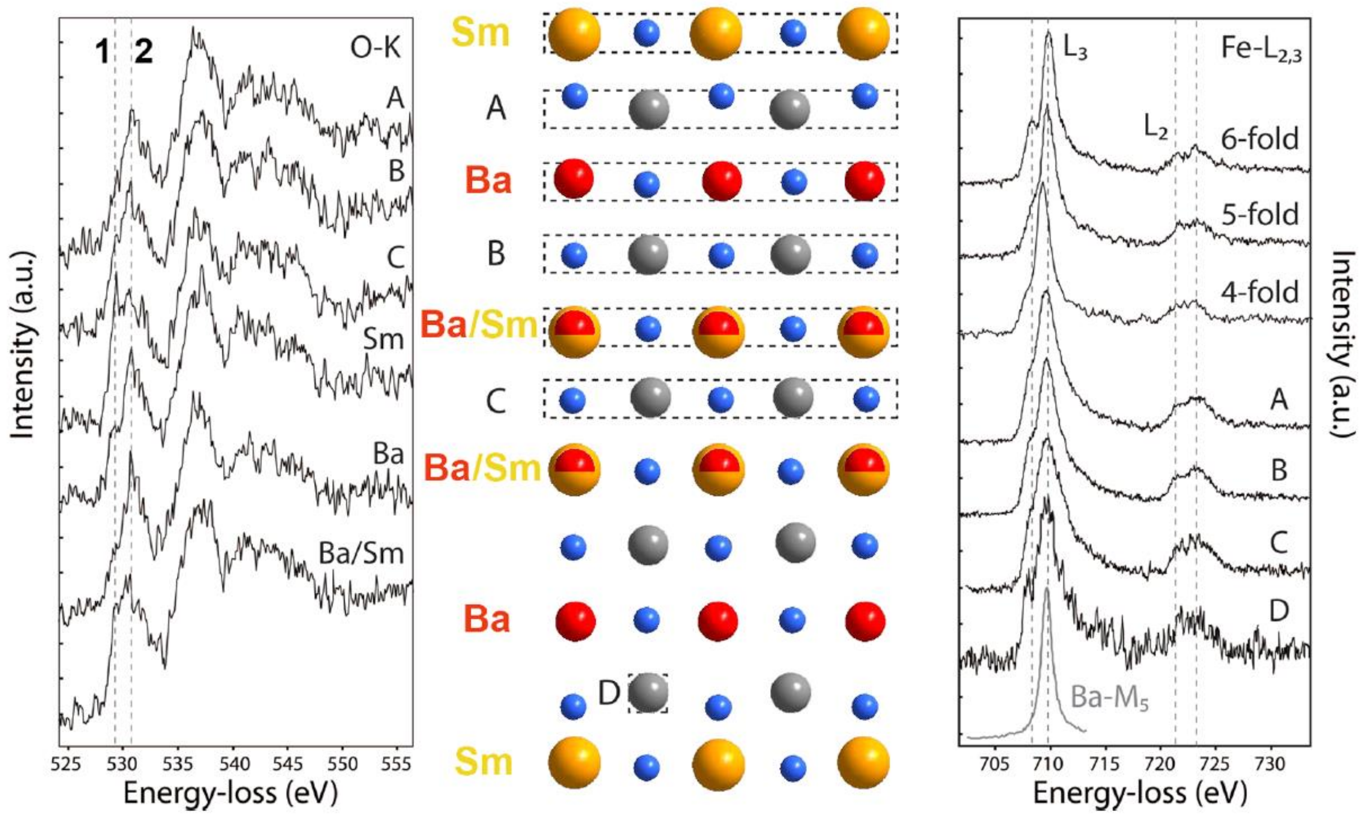

Figure 6. EELS fine structure of $Sm_{2-\varepsilon}Ba_{3+\varepsilon}Fe_5O_{15-\delta}$; (Left panel) O−K edge fine structure signatures from the regions indicated in the central panel. (Center panel) Structural model with indicated EELS integration areas. (Right panel) Fe-$L_{2,3}$ fine structure signatures from the regions indicated in the central panel with references for 4-, 5-, and 6-fold coordinated Fe^{3+}, and a simultaneously acquired and energy-shifted Ba M_5 edge.

NanoIndentation

Relatively new technique to obtain mechanical properties of nanometric regions

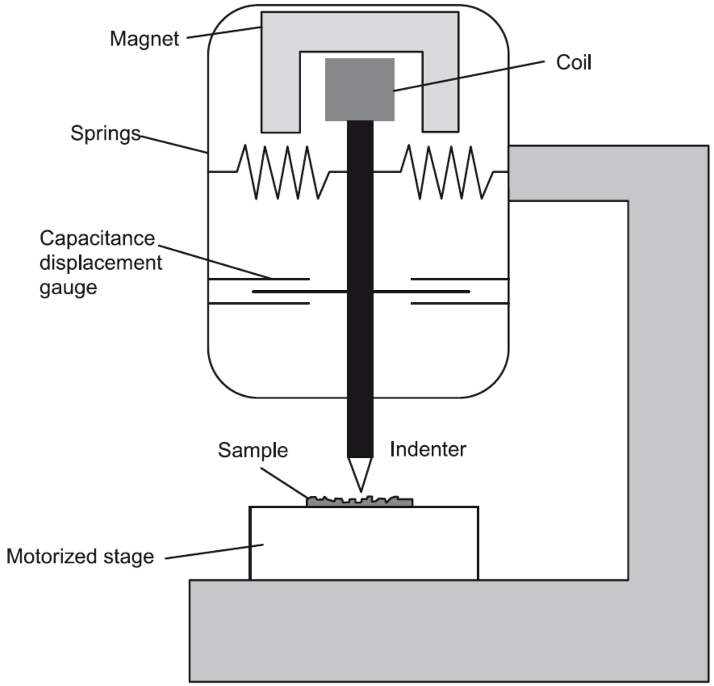

Fig. 5.15 Schematic diagram of nanoindentation mechanism.

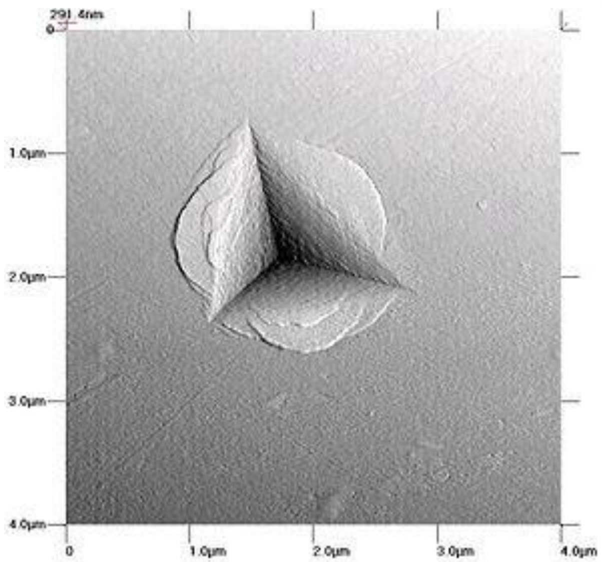

Zr-Cu-Al metallic glass

NanoIndentation

Load-displacement curve

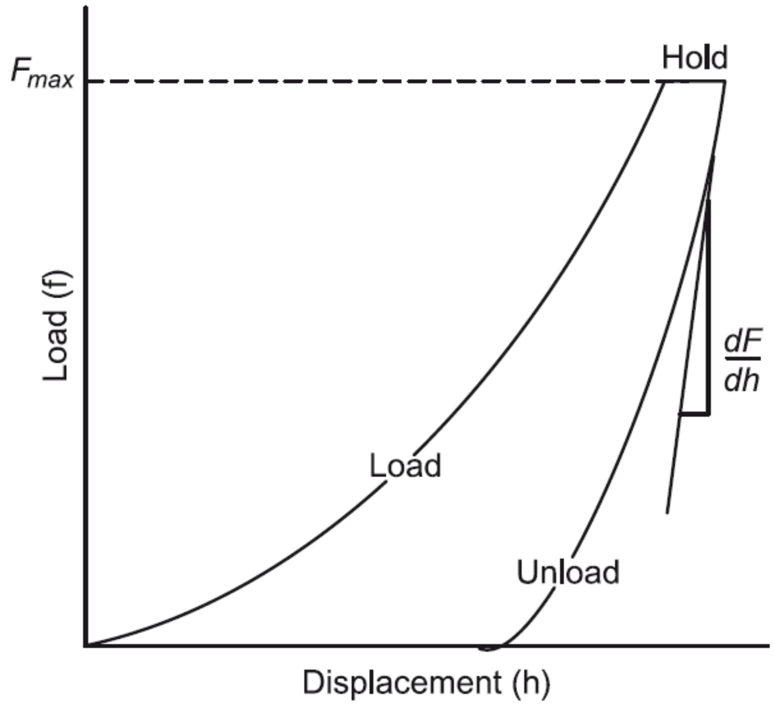

Fig. 5.16 Load–displacement curve of nanoindentation technique (*Source:* http://commons.wikimedia.org/wiki/File:Load-displacement_curve_%2B_onderdelen.JPG).

NanoIndentation

Zr-Pt alloy

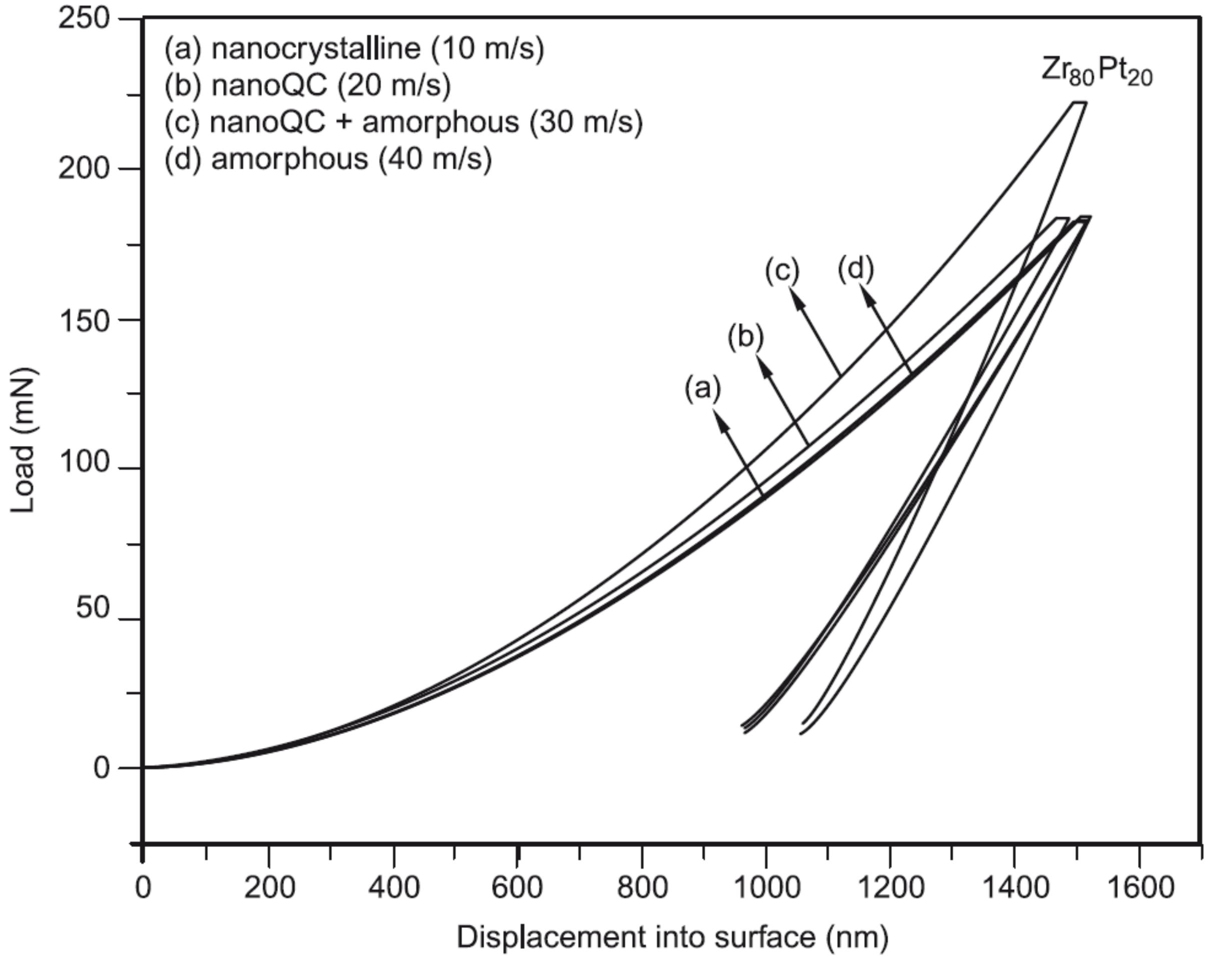

Fig. 5.17 Load–displacement curves for nanocrystalline Zr–Pt alloy (*Source:* BS Murty, IIT Madras).

NanoIndentation

Example

Journal of Power Sources 273 (2015) 522–529

Contents lists available at ScienceDirect

Journal of Power Sources

journal homepage: www.elsevier.com/locate/jpowsour

In-situ Young's moduli of the constitutive layers in a solid oxide fuel cell

Amit Pandey [a, b, *], Amit Shyam [a], Zhien Liu [b], Richard Goettler [b]

[a] Materials Science and Technology Division, Oak Ridge National Laboratory, Oak Ridge, TN 37831, USA
[b] LG Fuel Cell Systems Inc., North Canton, OH 44720, USA

H I G H L I G H T S

- A methodology to determine the modulus of functional layers in SOFCs is reported.
- *In-situ* Young's modulus for various functional layers is reported.
- The proposed testing methodology could be applied for other multilayer systems.

NanoIndentation

Example

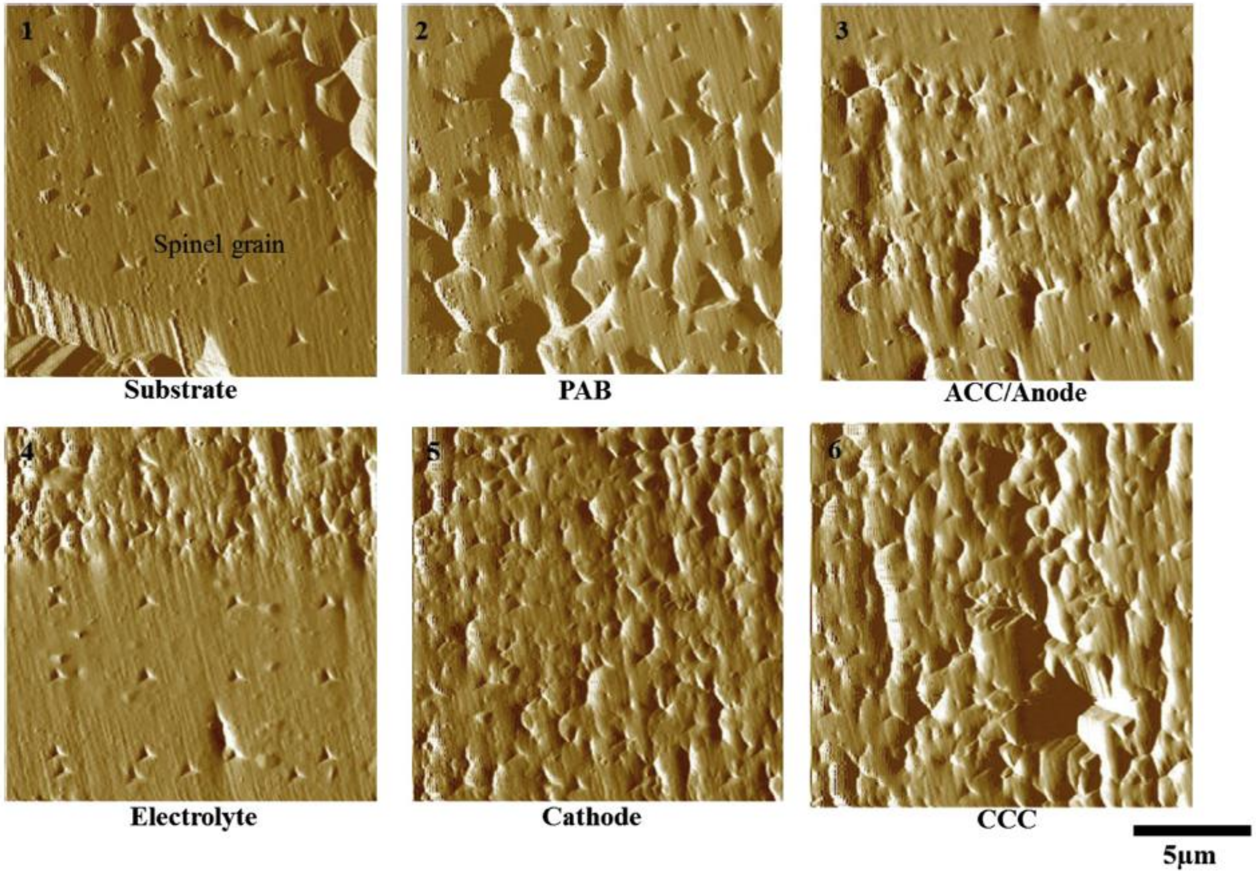

Fig. 5. Optical micrograph of typical nano indentation imprints on various layers in a substrate supported solid oxide fuel cell (SOFC).

NanoIndentation

Example

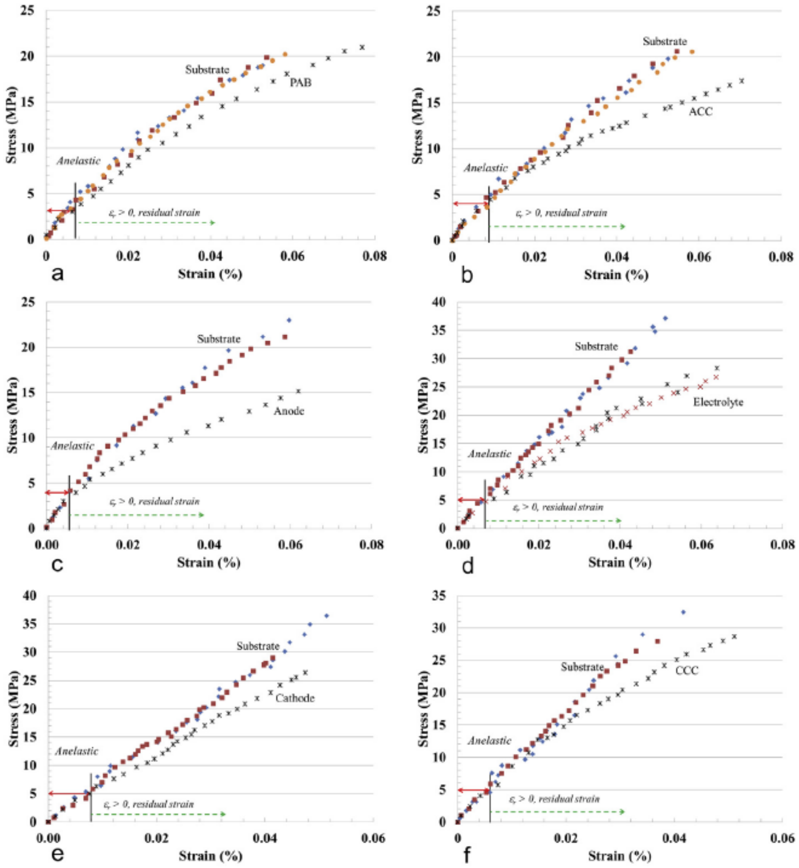

Fig. 4. a: Uniaxial monotonic tensile stress–strain response of bilayer specimen i.e. MMA substrate (S) + porous anode barrier (PAB). b: Uniaxial monotonic tensile stress-strain response of trilayer specimen i.e. MMA substrate (S) + porous anode barrier (PAB) + anode current collector (ACC). c: Uniaxial monotonic tensile stress–strain response of multilayer specimen i.e. MMA substrate (S) + porous anode barrier (PAB) + anode current collector (ACC) + anode (A). d: Uniaxial monotonic tensile stress-strain response of multilayer specimen i.e. MMA substrate (S) + porous anode barrier (PAB) + anode current collector (ACC) + anode (A) + electrolyte (E). e: Uniaxial monotonic tensile stress–strain response of multilayer specimen i.e. MMA substrate (S) + porous anode barrier (PAB) + anode current collector (ACC) + anode (A) + electrolyte (E) + cathode (C). f: Uniaxial monotonic tensile stress–strain response of multilayer specimen i.e. MMA substrate (S) + porous anode barrier (PAB) + anode current collector (ACC) + anode (A) + electrolyte (E) + cathode (C) + cathode current collector (CCC).

Summary

- Characterization of Nanomaterials: TEM, SEM, XPS, STM, AFM XRD, SAXS, EDX, EELS, Nanoindentation
  - Transmission/Scanning Electron Microscopy (TEM/SEM)
  - Scanning tunneling Microsopy
  - Atomic Force Microscopy
  - X-Ray Diffraction (XRD)
  - Small angle X-Ray scattering (SAXS)
  - Energy Dispersive X-Ray Spectroscopy (EDS/EDX)
  - Electron loss energy spectroscopy (EELS)
  - Nanoindentation
  - Many others: FIM, SPM, IR, RAMAN, HR-TEM, ED, SIMS, LEIS, ND, etc…